



U.S. DEPARTMENT OF
ENERGY

Office of
Science

DOE/SC-CM-20-002

FY 2020 Second Quarter Performance Metric: Evaluate Simulations of Mesoscale Convective Systems in E3SM v1 Water-Cycle Experiments

March 2020

DISCLAIMER

This report was prepared as an account of work sponsored by the U.S. Government. Neither the United States nor any agency thereof, nor any of their employees, makes any warranty, express or implied, or assumes any legal liability or responsibility for the accuracy, completeness, or usefulness of any information, apparatus, product, or process disclosed, or represents that its use would not infringe privately owned rights. Reference herein to any specific commercial product, process, or service by trade name, trademark, manufacturer, or otherwise, does not necessarily constitute or imply its endorsement, recommendation, or favoring by the U.S. Government or any agency thereof. The views and opinions of authors expressed herein do not necessarily state or reflect those of the U.S. Government or any agency thereof.

Contents

1.0 Product Definition	1
2.0 Product Documentation	1
3.0 Results	2
4.0 References	7

Figures

Figure 1. A schematic illustration of the FLEXTRKR MCS tracking algorithm using criteria for cold cloud systems (a) and precipitation features (b) to track MCSs and their evolution (c).	2
Figure 2. Observed and E3SM simulated total precipitation (a and d), MCS precipitation (b and e), and ratio of MCS-to-total precipitation (c and f) during spring (MAM) east of the Rocky Mountains in the U.S.	3
Figure 3. Similar to Figure 2, but for summer (JJA).	3
Figure 4. Observed and simulated MCS number (a and d), MCS rain frequency (b and e), and MCS rain intensity (c and f) during spring.	4
Figure 5 Similar to Figure 4, but for summer.	4
Figure 6. Climatological average numbers of MCSs in the central U.S. from observation (blue) and simulation (orange) between March and August.	5
Figure 7. Observed (blue) and simulated (orange) PF diameter (a and b), PF mean rain-rate (c and d) and PF volumetric rain-rate (e and f) as a function of the normalized MCS lifecycle (x-axis) during spring (left) and summer (right) averaged over the central US.	5
Figure 8. Diurnal cycle of MCS (solid) and non-MCS (dashed) precipitation averaged over the central U.S. from observation (blue) and simulation (orange) during spring (a and c) and summer (b and d). Actual precipitation amounts are shown in (a and b) and normalized precipitation amounts are shown in (c and d).	6

1.0 Product Definition

Mesoscale convective systems (MCSs) consist of an assembly of cumulonimbus clouds on scales of 100 km or more and produce mesoscale circulations (Houze 2004, 2018). As the largest form of deep convective storms, MCSs contribute to 30%–70% of annual and warm season rainfall as well as over half of the extreme daily rainfall events in the U.S. east of the Rocky Mountains (Stevenson and Schumacher 2014, Feng et al. 2019, Haberlie and Ashley 2019). MCSs are notoriously difficult to simulate in global climate models (GCMs). Failure in simulating MCSs in the Central U.S. is manifested in the erroneous diurnal cycle of precipitation and large warm bias in the near-surface temperature (Lin et al. 2017).

The Energy Exascale Earth System Model (E3SM) has been developed to support the U. S. Department of Energy (DOE)'s energy mission by providing an improved capability to predict future changes in the water cycle, biogeochemical cycle, and cryosphere systems that affect energy production and use. As part of the water-cycle experiments, E3SM v1 has been configured at low (~ 100 km) and high (~ 25 km) resolution to evaluate the impacts of model resolution on simulating water-cycle processes such as precipitation, snowpack, and runoff (Caldwell et al. 2019). This document summarizes analyses performed to evaluate a high-resolution E3SM simulation at 25-km resolution, focusing particularly on its ability to reproduce the observed MCSs and their characteristics in the central U.S. An MCS tracking algorithm is applied to both observations and the model simulation and various features such as MCS number, rain frequency and intensity, and their variability at seasonal and diurnal timescales are evaluated. As the resolution of E3SM continues to increase in the future, evaluating the model skill in simulating MCSs over multiple versions with improved physics parameterizations and model resolution is important for documenting progress towards advancing modeling of water-cycle processes in E3SM.

2.0 Product Documentation

As part of the water-cycle experiments, E3SM v1 has been used to perform simulations using a low-resolution (LR) and a high-resolution (HR) configuration following the Coupled Model Intercomparison Project Phase 6 (CMIP6) HighResMIP protocol (Haarsma et al. 2016). The LR and HR configurations feature the atmosphere and land models at ~100-km and ~25-km grid spacing and the ocean and sea ice models at 30–60-km and 6–18-km grid spacing, respectively. In the control simulations of HighResMIP, time-invariant 1950 forcings are prescribed. Caldwell et al. (2019) reported analysis and comparison of two 50-year control simulations at LR and HR. In these simulations, the ocean and sea ice were initialized based on standalone simulations of the E3SM ocean and sea ice models driven by climatological atmospheric forcing. The HR simulation was then extended for 20 years to archive high-frequency model output, including hourly precipitation and 6-hourly, three-dimensional atmospheric temperature, moisture, and winds, among other variables. These high-frequency results are analyzed and evaluated in this document.

To evaluate the E3SM HR simulation of MCSs, the FLEXTRKR algorithm (Feng et al. 2018, 2019) is used to identify and track MCSs in both simulation and observations. An MCS is defined as a large cold cloud system (CCS) with brightness temperature (T_b) < 241 K and an area exceeding 6×10^4 km² that contain a precipitation feature (PF) with major axis length > 100 km. Furthermore, the PF area, mean rain rate, and rain rate skewness must be larger than the lifetime-dependent thresholds. An MCS is

tracked when both conditions of CCS and PF are met continuously for longer than six hours. For the E3SM HR simulation, hourly precipitation and outgoing longwave radiation are used to track MCSs. For observations, hourly satellite infrared data and Next-Generation Radar Network (NEXRAD) precipitation data for 2004–2016, coarsened to 25-km resolution, are used to track MCSs for comparison. A schematic illustration of MCS tracking using FLEXTRKR is shown in Figure 1. As MCS features are not well defined at 100-km grid spacing, only the E3SM HR simulation is analyzed and reported here.

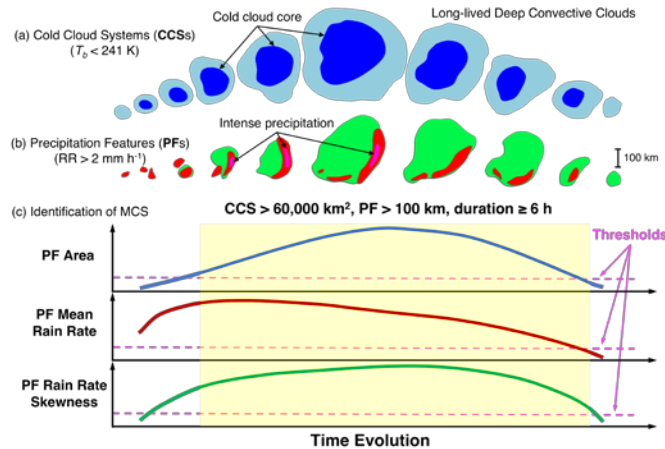


Figure 1. A schematic illustration of the FLEXTRKR MCS tracking algorithm using criteria for cold cloud systems (a) and precipitation features (b) to track MCSs and their evolution (c).

3.0 Results

MCSs occur frequently in spring and summer east of the Rocky Mountains. Figure 2 compares the observed and simulated total precipitation, MCS precipitation, and the ratio of MCS to total precipitation during spring (March–April–May) when the passage of strong baroclinic waves provides a lifting mechanism for initiation of MCSs in the central U.S. (Song et al. 2019, Feng et al. 2019). E3SM generally captures the east–west gradient of total precipitation, but the amount is slightly underestimated and shifted to the east. Although the total precipitation is quite well simulated, the model significantly underestimates MCS precipitation, which contributes to 30–70% of the observed total precipitation in the Great Plains. In the model, MCS precipitation contributes to no more than 40% of the total precipitation.

Similar to Figure 2, Figure 3 compares the observed and simulated total and MCS precipitation during summer (June–July–August). Compared to spring, the maximum total precipitation shifts poleward to the northern Great Plains and becomes stronger and more widespread in the southern and eastern coastal regions in the observations (Figures 2a and 3a). E3SM exhibits a larger underestimation in summer than spring, with no obvious poleward shift as evident from the observations. MCS precipitation is more significantly underestimated by the model in summer than spring, which is noticeable from the larger bias in the ratio of MCS to total precipitation in summer when MCS generally accounts for 20%–30% and 30%–70% of the total precipitation in the simulation and observations, respectively. Song et al. (2019) noted that MCSs in the central U.S. are less predictable in summer than spring because they are less frequently associated with synoptic-scale forcing in the summer.

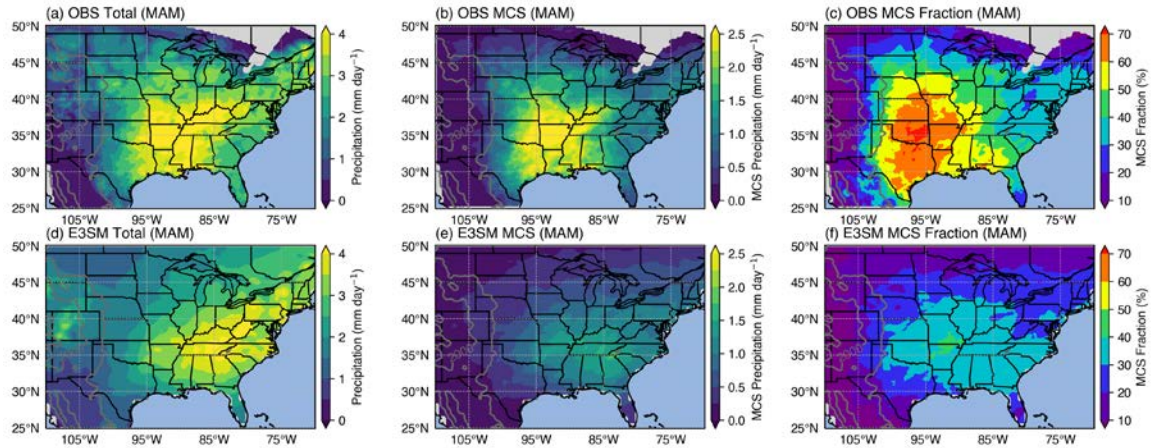


Figure 2. Observed and E3SM-simulated total precipitation (a and d), MCS precipitation (b and e), and ratio of MCS to total precipitation (c and f) during spring (MAM) east of the Rocky Mountains in the U.S.

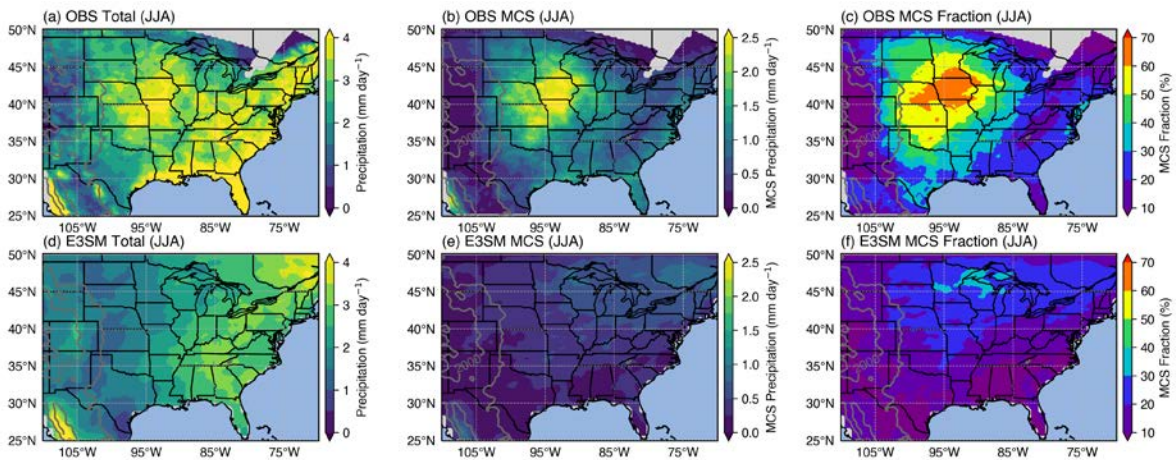


Figure 3. Similar to Figure 2, but for summer (JJA).

By tracking MCSs in observations and simulations, we can also evaluate how well the model simulates the number, rain frequency, and rain intensity of MCSs. The observed spatial distributions of the MCS number and rain frequency display similar features as the MCS precipitation, showing a notable northward shift from spring to summer. In contrast, MCS rain intensity has a more uniform spatial distribution, with higher intensity in summer than spring in the observations. The number and rain frequency of MCSs in spring are well simulated except for the eastward shift as noted earlier. MCS rain intensity, however, is underestimated, leading to an overall underestimation of MCS precipitation in spring (Figure 2). Larger biases are notable in the summer season in all three aspects, number, rain, and intensity, of MCSs (Figure 5). Comparing the model-observation differences in MCS rain frequency and rain intensity, it is clear that the model bias in MCS rain intensity has a larger contribution than MCS rain frequency to the model underestimation of MCS precipitation.

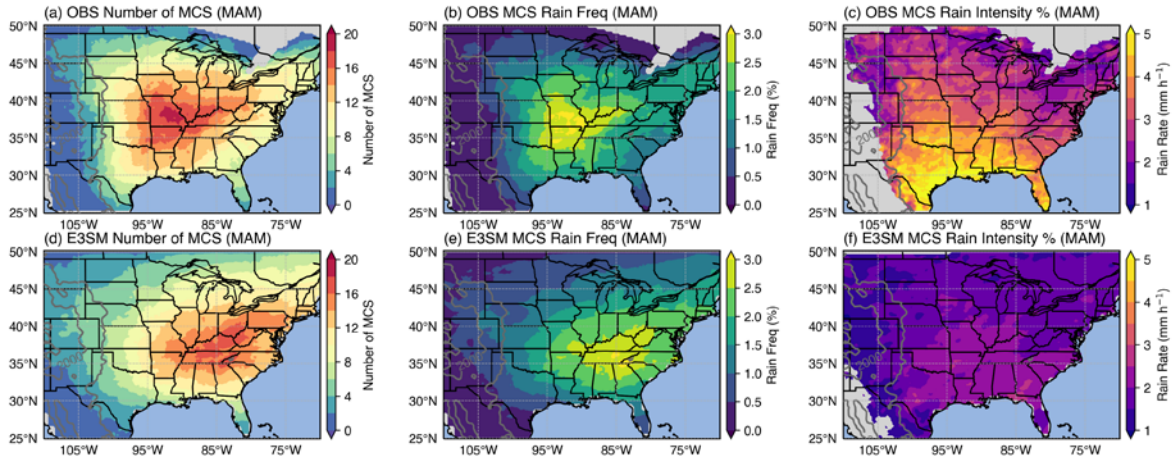


Figure 4. Observed and simulated MCS number (a and d), MCS rain frequency (b and e), and MCS rain intensity (c and f) during spring.

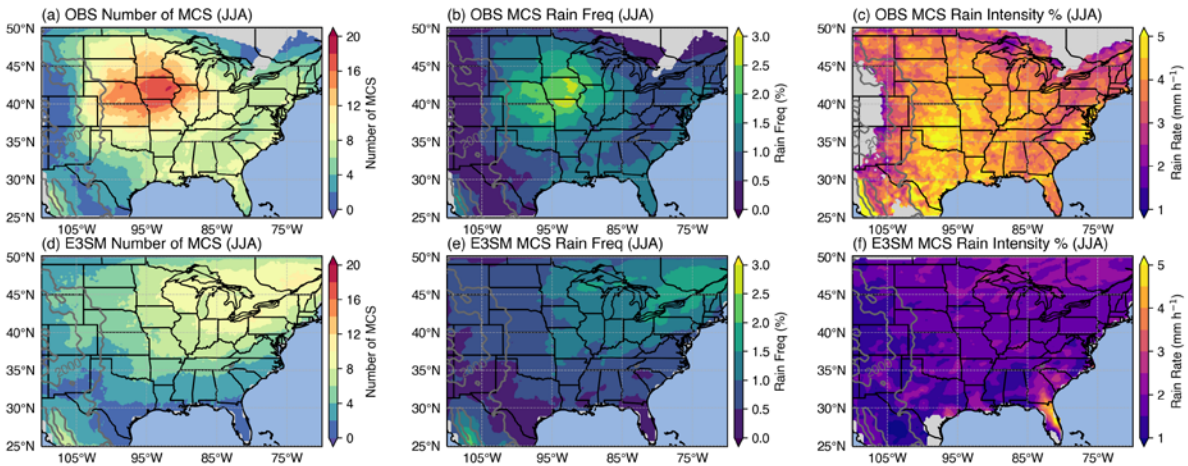


Figure 5 Similar to Figure 4, but for summer.

The analysis shown in Figures 4 and 5 can be summarized by comparing the averages over the central U.S. Figure 6 shows the seasonal cycle of the total number of MCSs averaged over the observation and simulation periods. MCS occurrence increases from March and peaks in June in the observation. Due to the larger underestimation of MCS number in summer than spring, the simulated MCS number peaks in May and decreases from June to August more rapidly than observation. The biases in MCS rain intensity are also summarized in Figure 7 by comparing the observed and simulated MCS size in terms of the PF diameter and PF mean rain rate. The simulated MCS PF area is slightly larger than the observed, but the simulated PF mean rain rate is significantly lower than observed, especially at the early stage of the MCS life cycle. As a result, the PF volumetric rainfall is about half of the observed in both spring and summer.

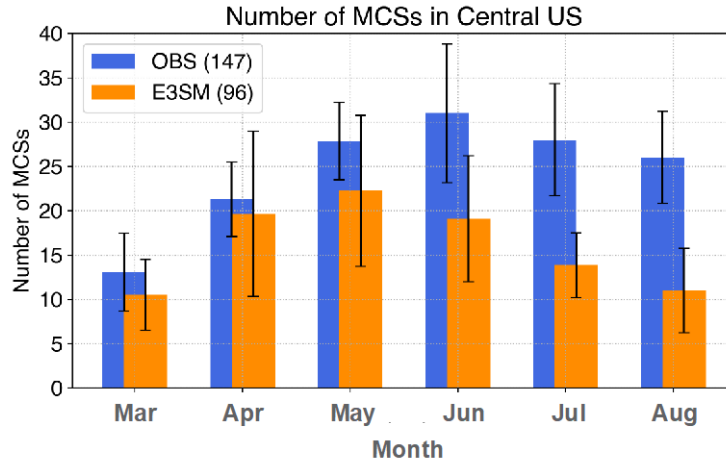


Figure 6. Climatological average numbers of MCSs in the central U.S. from observation (blue) and simulation (orange) between March and August.

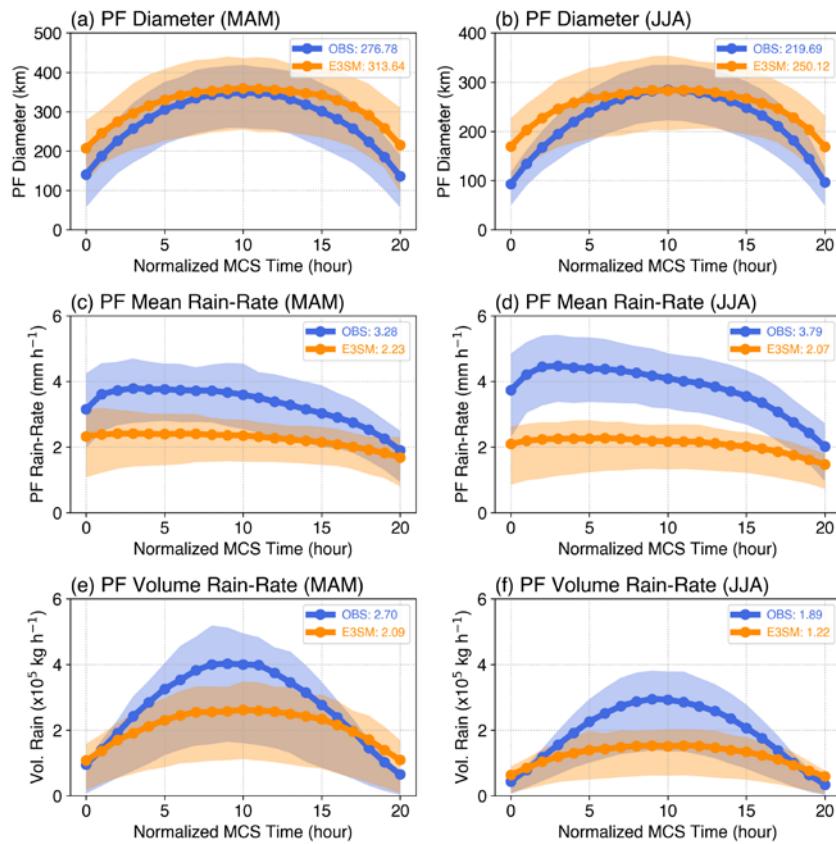


Figure 7. Observed (blue) and simulated (orange) PF diameter (a and b), PF mean rain-rate (c and d), and PF volumetric rain-rate (e and f) as a function of the normalized MCS life cycle (x-axis) during spring (left) and summer (right) averaged over the central U.S.

A distinguishing feature of MCS precipitation relative to non-MCS precipitation is its diurnal timing. In the observations, MCS precipitation averaged over the central U.S. displays a nocturnal peak at around midnight in both spring and summer while non-MCS precipitation peaks around 6 pm (Figure 8). With

stronger solar forcing, the diurnal amplitude is much stronger in summer than spring. Averaged over the day, MCS and non-MCS precipitation contribute almost equally in amount to the total precipitation. In contrast, non-MCS precipitation dominates the total precipitation in the simulation during both spring and summer. The model realistically simulates the 6 pm peak for non-MCS precipitation particularly in spring, while afternoon precipitation is distributed more evenly between noon and 6 pm in summer. For MCS precipitation, the diurnal peak is shifted towards early morning in the simulation relative to midnight in the observation, but the delay is notably smaller in spring than summer. The diurnal timing is more clearly depicted by the normalized precipitation (i.e., ratio of hourly to daily precipitation) as the simulated diurnal amplitude of MCS precipitation is only ~10% of the observed.

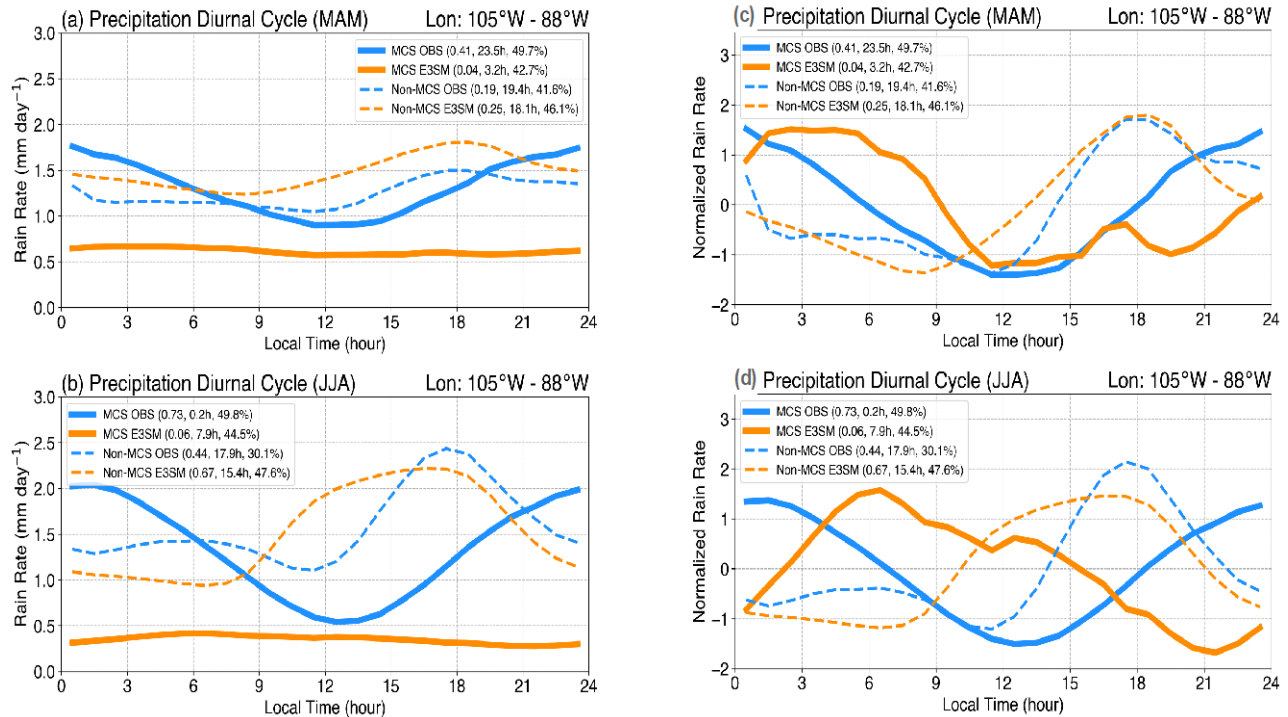


Figure 8. Diurnal cycle of MCS (solid) and non-MCS (dashed) precipitation averaged over the central U.S. from observation (blue) and simulation (orange) during spring (a and c) and summer (b and d). Actual precipitation amounts are shown in (a and b) and normalized precipitation amounts are shown in (c and d).

In summary, an MCS tracking algorithm has been applied to observations and an E3SM HR simulation at 25-km grid spacing to evaluate MCS precipitation characteristics simulated by the model. The model is generally more skillful in simulating both the total and MCS precipitation in spring than summer. The spring-summer contrast in model skill is consistent with the environments that support MCS development in the two seasons: synoptic-scale activities in spring and smaller-scale perturbations in summer, suggesting less predictability for MCSs in the summer. Therefore, even in convection-permitting regional simulations at 4-km grid spacing without a cumulus parameterization, Prein et al. (2017) reported degraded skill in simulating MCSs in summer relative to spring over the central U.S.

E3SM shows some obvious deficiency in simulating MCS precipitation intensity in both spring and summer. Also notably, MCSs in the model are slightly too large, with significantly lower mean rain-rate than those in the observation, resulting in large underestimation of MCS volumetric rain-rate. The model

is able to realistically simulate the late afternoon peak for non-MCS precipitation, but for MCS precipitation the peak is delayed by up to six hours and the amplitude is only about 10% of the observed. These model biases are likely related to both the cumulus parameterization and microphysics parameterization used in the model, with the former having important effect on the diurnal cycle of precipitation and the latter having important effect on the MCS PF size and rain-rate. Biases in simulating the stratiform rain of MCSs has important effect on the diabatic heating profile, with positive feedback to the strength and longevity of MCSs (Yang et al. 2017, Feng et al. 2018). Through the positive feedback between the diabatic heating profile and MCS strength, even small biases in simulating the large-scale environment may amplify the biases in simulating MCS characteristics. The contributions of biases in the large-scale environment to model biases in MCS precipitation will be investigated using the 6-hourly 3D atmospheric variables archived from the E3SM HR simulation. Understanding the relative contributions of large-scale circulation biases versus biases associated with the cumulus and cloud microphysical parameterizations will provide useful guidance for improving the ability of E3SM in modeling MCS, which is a key element of the regional and global water cycle.

4.0 References

- Caldwell, PM, A Mamejtanov, Q Tang, LP Van Roedel, J-C Golaz, W Lin, DC Bader, ND Keen, Y Feng, R Jacob, ME Maltrud, AF Roberts, MA Taylor, M Veneziani, H Wang, JD Wolfe, K Balaguru, P Cameron-Smith, L Dong, SA Klein, LR Leung, H-Y Li, Q Li, X Liu, RB Neale, M Pinheiro, Y Qian, PA Ullrich, S Xie, Y Yang, Y Zhang, K Zhang, and T Zhou. 2019. “The DOE E3SM coupled model version 1: Description and results at high resolution.” *Journal of Advances in Modeling Earth Systems* 11(12): 4095–4146, <https://doi.org/10.1029/2019MS001870>
- Feng, Z, LR Leung, RA Houze, S Hagos, J Hardin, Q Yang, 2018. “Structure and Evolution of Mesoscale Convective Systems: Sensitivity to Cloud Microphysics in Convection-Permitting Simulations over the United States.” *Journal of Advances in Modeling Earth Systems* 10(7): 1470–1494, <https://doi.org/10.1029/2018MS001305>
- Feng, Z, RA Houze, LR Leung, F Song, JC Hardin, J Wang, WI Gustafson, and CR Homeyer. 2019. “Spatiotemporal Characteristics and Large-Scale Environments of Mesoscale Convective Systems East of the Rocky Mountains.” *Journal of Climate* 32(21): 7303–7328, <https://doi.org/10.1175/JCLI-D-19-0137.1>
- Haarsma, RJ, MJ Roberts, PL Vidale, CA Senior, A Bellucci, Q Bao, P Chang, S Corti, NS Fuckar, V Guemas, J von Hardenberg, W Hazeleger, C Kodama, T Koenigk, LR Leung, J Lu, J-J Luo, J Mao, MS Mizieliński, R Mizuta, P Nobre, M Satoh, E Scoccimarro, T Semmler, J Small, and J-S von Storch. 2016. “High Resolution Model Intercomparison Project (HighResMIP v1.0) for CMIP6.” *Geoscientific Model Development* 9(11): 4185–4208, <https://doi.org/10.5194/gmd-9-4185-2016>
- Haberlie, AM, and WS Ashley. 2019. “A Radar-Based Climatology of Mesoscale Convective Systems in the United States.” *Journal of Climate* 32(5): 1591–1606, <https://doi.org/10.1175/JCLI-D-18-0559.1>
- Houze, RA. 2004. “Mesoscale convective systems.” *Review of Geophysics* 42(4): RG4003, <https://doi.org/10.1029/2004RG000150>

Houze, RA. 2018. “100 years of research on mesoscale convective systems.” *Meteorological Monographs* 59: 17.1–17.54. <https://doi.org/10.1175/AMSMONOGRAPHS-D-18-0001.1>

Lin, Y, W Dong, M Zhang, Y Xie, W Xue, J Huang, and Y Luo. 2017. “Causes of model dry and warm bias over central U.S. and impact on climate projections.” *Nature Communications*, 8(1): 881, <https://doi.org/10.1038/s41467-017-01040-2>

Prein, AF, C Liu, K Ikeda, R Bullock, RM Rasmussen, GJ Holland, and M Clark. 2017. “Simulating North American mesoscale convective systems with a convection-permitting climate model.” *Climate Dynamics* <https://doi.org/10.1007/s00382-017-3993-2>

Song, F, Z Feng, LR Leung, RA Houze Jr, J Wang, J Hardin, and CR Homeyer. 2019. “Contrasting Spring and Summer Large-Scale Environments Associated with Mesoscale Convective Systems over the U.S. Great Plains.” *Journal of Climate* 32(20): 6749–6767, <https://doi.org/10.1175/JCLI-D-18-0839.1>

Stevenson, SN, and RS Schumacher. 2014. “A 10-Year Survey of Extreme Rainfall Events in the Central and Eastern United States Using Gridded Multisensor Precipitation Analyses.” *Monthly Weather Review* 142(9): 3147–3162, <https://doi.org/10.1175/MWR-D-13-00345.1>

Yang, Q, RA Houze Jr, LR Leung, and Z Feng. 2017. “Environments of long-lived mesoscale convective systems over the central United States in convection permitting climate simulations.” *Journal of Geophysical Research – Atmospheres* 122(24): 13288–13307, <https://doi.org/10.1002/2017JD027033>



U.S. DEPARTMENT OF
ENERGY

Office of Science